The influence of phase mask position upon EDoF system

Sheng-Hsun Hsieh[a], Zih-Hao Lian[a], Chong-Min Chang[b] and Chung-Hao Tien[a]
[a]Department of Photonics, National Chiao Tung Univ./Hsinchu, Taiwan;
[b]MaxEmil Photonics Corp./Taipei, Taiwan

ABSTRACT

Special types of pupil mask with the appropriate phase and transmission distribution can be used to modify the 3D point-spread function (PSF) in the desired way. Recently, many studies were addressed to extend the depth-of-field (EDoF) of an imaging system via cubic phase pupil engineering. The intermediate image is detected with a digital sensor and the final image formation is restored by post-process algorithms with the help of knowledge of the pupil mask. The EDoF system is operated based on an assumption that the phase mask should be positioned exactly in the pupil of the optical system. Unfortunately, in most practical cases, the exit pupil is not always available due to the complex layout of a compound lens set and results in a limited practical benefit of this type of arrangement. In this paper, we present the influence of the phase mask position upon PSF of an extended depth-of-field system. The characterizations of EDoF in different viewing angles are dissimilar if the phase mask is not placed in the perfect pupil plane. Such properties should be taken into consideration while designing an EDoF system. Finally, we will propose some potential candidate lenses made to alleviate such difficulty.

Keywords: point-spread function, extended depth-of-field, cubic phase mask

1. INTRODUCTION

It's well known that the complex pupil function has a strong influence on the form of the point spread function (PSF) as well as the modulation transfer function (MTF) of an imaging system. Therefore, PSF manipulation for special purposes was developed by the so called pupil engineering [1]. Recently, extended depth of field (EDoF) technique attracts much attention due to its unique feature in ultra-high axial resolution resistance to defocus without sacrifice of transverse resolution [2]. In principle, there are two approaches to attempt EDoF function. In the first case, all-optical-elements in a passive way, the shaped 3D caustic are designed directly for image formation by means of the spatial pupil masks, such as multi-zone complex pupil filter, Toraldo and Axicon optical element [3-4]. In the second and more complex way, the intermediate image is detected with a digital sensor and the final image formation is calculated by the post-process algorithms with the help of the knowledge of the pupil mask. Such digital image formation offers the possibility of generating quite new imaging aspects. Dowski and Cathey proposed to use a cubic phase curve to enable the system MTF at a stationary point [5-7]. The pupil mask generates an intermediate image of poorer quality by an asymmetric triangular PSF, but after deconvolution of the digital detected image with the known Wiener filter which can be restored is independent of the defocus in a certain range. The system is operated based on the assumption that the elaborated PSFs are kept identical through a certain range of focus. For practical use, however, the engineered phase masks are difficult to be placed exactly in the pupil plane because the pupil is not always physically available within the compound lenses set. The question arises that if the phase mask was placed at anywhere other than the pupil plane, will the restored image be deteriorated due to the PSF variation? In this study, we will address the characteristics of EDoF system and quantitatively analyze the influence between exit pupil and aperture stop coding. Finally, some potential solutions are proposed to overcome this issue.

2. PUPIL ENGINEERING

For a perfect imaging system, it is required that all light rays emitted from an object point would meet at an ideal image point. All light paths between object and conjugate image points have the same optical path length. For image formation, the entrance pupil is the image of the aperture stop in the object space, whereas the aperture stop is a physical limitation of an imaging system. From the viewpoint of wave optics, the aperture stop physically constrains the angular spectrum passing through the optical system, thus determining the imaging bandwidth of the canonical conjugates in an imaging

Novel Optical Systems Design and Optimization XVI, edited by G. Groot Gregory,
Arthur J. Davis, Proc. of SPIE Vol. 8842, 884207 · © 2013 SPIE
CCC code: 0277-786X/13/$18 · doi: 10.1117/12.2023500

system. Likewise, the exit pupil is given by the image of the aperture stop in image space. As shown in Figure 1, both pupils are the canonical pupils of an optical system. Since the aperture stop physically limits ray bundles propagating through the optical system, and thus limits the optical direction cosines passing from object space to image space, the aperture stop plays an essential role in governing the point spread function of image formation. Consequently, the image intensity is determined by the convolution of the object intensity distribution with the point-spread function. Optical imaging is considered a linear transformation system. Therefore, many studies were dedicated to engineer the imaging performance by the specific modulation at the canonical pupil planes.

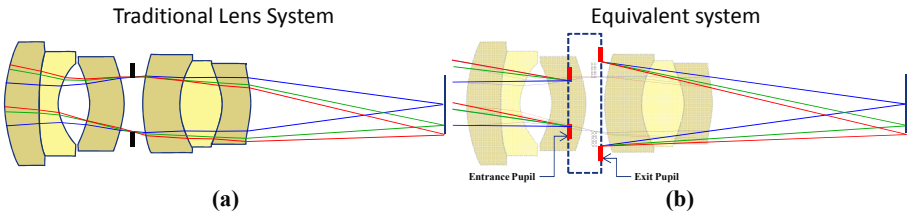

Figure 1. (a) A camera system is composed of several lenses and aperture stop (b) Equivalent system as a black box consist of entrance pupil and exit pupil.

The pupil filter is usually constructed as a complex mask with phase or absorbing effects. Generally, a pure imaginary phase filter is more popular due to its inherently high transmission. In this case, the greatest degrees of wavefront design can be used to shape the focal caustic. The structuring of the pupil function to modify the PSF or MTF is sometimes called wavefront coding. Unfortunately, in most practical cases, the pupils are not all physically available. As shown in Figure 2, the aperture stop is embedded amid the compound lens set and is hard to be coded. The entrance and exit pupils are not physically available due to their position are coinciding with real entities. Most research implements wavefront coding by putting the phase filter at front or rear space of the system. In this paper, we investigated the position of a phase mask highly influencing the system PSF as well as the restoration process for digital optics. More detail and discussions will be included in section 2.4.

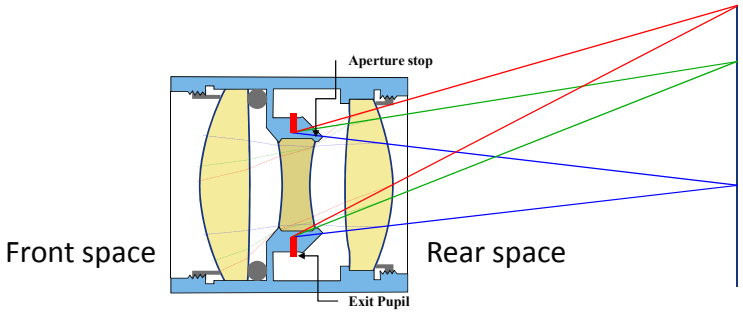

Figure 2. An example of failure for phase mask position, where the position of the aperture stop and exit pupil both collide with the mechanism, and are physically unavailable.

2.1 Extended Depth of field and Cubic Phase Mask

There are several possible ways to determine pupil phase filters for special purposes concerned with the modification of the PSF in three dimensions. There have been many studies about the optimization criterion for the fundamental limits of resolution and the caustic parameters, which can be deduced from simple analytical treatment of the diffraction integral and Fourier optics [9]. According to prior literature, we would keep the uniform axial distribution of the PSF, and a radially symmetric phase mask with spherical aberration can be obtained. On the other hand, for transfer function, Dowski and Cathey proposed a cubic phase mask of an imaging system to enable the MTF to have a stationary point. In order to avoid the information loss, the MTF with wavefront coding should have no null points. With the post-process algorithms such as a Wiener-Kolmogorov filter, the intermediate image detected by a digital sensor can be restored into the final image with decent quality. In this paper, we represent a cubic phase profile as a test case [5]:

$$P(\xi,\eta)=\exp\left[i\alpha\left(\xi^3+\eta^3\right)\right] \tag{1}$$

where P(ξ,η) is the pupil function and the indices ξ, η are the normalized coordinates in the pupil plane. The choice of coding strength value, α, governs the coding strength of the mask. The phase element should balance a trade-off between sharpness at the optimal focus position and the variation of the blur spot with respect to different object distance. The proposed procedure to find the appropriate α value follows: firstly, derive the aperture and the minimal MTF value needed for the predefined image merit figure, then optimize α by minimizing the mean square error (MMSE) between ideal and defocus coded images. Secondly, MTF of a coded system cannot cross zero value due to the reason that the null point in MTF will lead to information loss and no longer be restored by post processing. Thirdly, the lens manufacturing tolerance should be considered to avoid the coincidence between optomechanical setup and ideal phase as showing the case in Figure 2. Refer to the appropriate MTF value at Nyquist frequency of the wavefront coding scheme, the minimum MTF at Nyquist frequency in this study was set as 0.149 [6-7].

2.2 Geometric Modeling

In order to practically consider the phase mask and conduct ray-tracing analyses, it's inadequate to neglect the thickness of the phase mask as prior studies. Tiny shifts of ray position would lead to a severe aberration and affect the wave front coding, resulting in the underperformance of an EDoF system. In this section, we built up a first-order geometric model of the phase mask to deduce the PSF via a ray tracing scheme. As a simplification, the exit pupil of an optical system is frequently described as the plane from which to converge a bundle of rays at a distance z_i. Here we decompose the cubic phase mask into two parts: flat glass and phase glass. Figure 3 (a) shows the convergent light travelling through a flat glass on exit pupil with thickness d. The focal plane has a displacement (d - d/n). Our goal is to derive the transverse shift emitted from flat glass to a new focal plane ($z_i + \Delta z$ - d). Based on first order approximation and Snell's Law, transverse shift T_g emitted from flat glass to a new focal plane can be given by Eq. (2):

$$T_g = (z_i + \Delta z - d) \times \theta_o = -x\left(1 - \frac{d}{nz_i}\right) \tag{2}$$

Figure 3 (b) shows the convergent ray through a one dimensional cubic phase mask with thickness d. The surface profile is given by Ax^3, in which the surface profile coefficient A is different from the coding strength α in phase expression in Eq. (1). The coefficient A is a general coordinate relevant to physical pupil size and α is a normalized coordinate ranging from 0 to 1. The incident angle, $\theta_i = (-x)/z_i$, was refracted by the lens to angle $\theta = \theta_i/n$. The cubic surface deviates the ray by derivative of $\Delta\theta = 3Ax^2$, so the output angle is $\theta_o = n(\theta+\Delta\theta)-\Delta\theta$. The transverse shift T_{shift} emitted from flat glass to the new focal plane can thus be given by Eq. (3)

$$T_{shift} = (z_i + \Delta z - d) \times \theta_o = -x\left(1 - \frac{d}{nz_i}\right) + 3\left(z_i - \frac{d}{n}\right)(n-1)Ax^2 = T_g + T_p \tag{3}$$

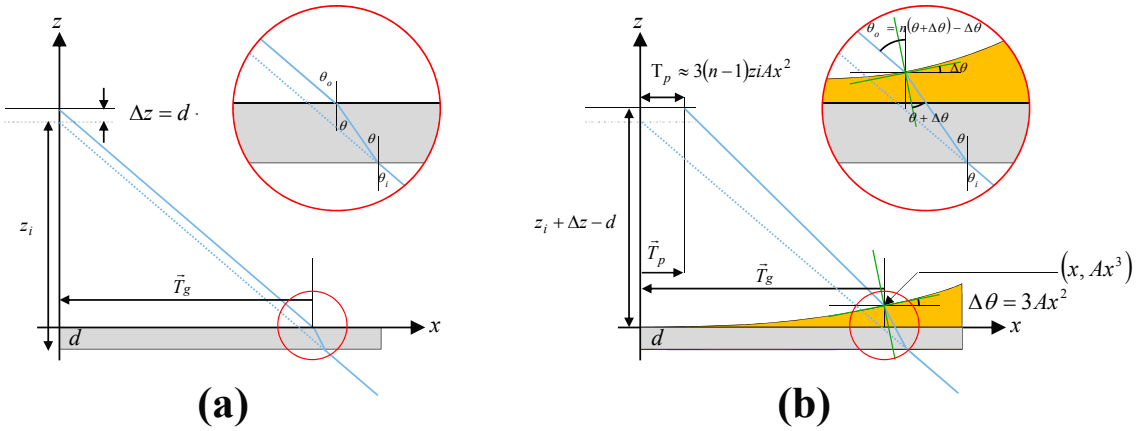

Figure 3. First order geometric model (a) flat glass with thickness d (b) cubic phase mask composition to flat subtract in thickness d and phase term Ax^3.

The result was divided into two parts, flat glass term (T_g) contributes to focus all the light rays to a point and phase glass term (T_p) represents a lateral shift to the light rays. As the thickness d is much less than imaging distance z_i, T_p is approximated as shown in below Eq. (4)

$$T_p \approx 3(n-1)z_i Ax^2 \tag{4}$$

Eq. (4) presents many insights for the features of a phase mask, where the PSF (or focal spot) of a cubic phase profile are proportional to three factors: surface profile coefficient A, imaging distance z_i and the square of pupil size, respectively.

2.3 The Characteristics of Pupil Modulation

In this section, we validate the preceding geometric derivation with Fourier analysis. The phase profile can be represented as $P(\xi) = \exp[i\alpha(x/w)^3] = \exp[ink_0 z]$. Where w is the half width of clear aperture and n is the refractive index of the mask material. Sag of the lens surface can be derived as $sag(z) = \alpha\lambda_0/2\pi n\times(x/w)^3 = Ax^3$, the surface profile coefficient A is given by $\alpha\lambda_0/2\pi nw^3$. T_p can be rewritten as

$$T_p \approx \frac{3(n-1)\lambda_0}{2\pi\pi}\times\frac{\alpha z_i}{w} \tag{5}$$

After the coordinate normalization, the focal spot size can be obtained in viewpoint of wave optics. The complex amplitude transmittance through cubic phase mask is given by [10]

$$t(x,y) = \exp\left[i(1-1/n)\alpha\left(\xi^3+\eta^3\right)\right] \tag{6}$$

Modified pupil function as Eq. (6) has an additional scale factor (1-1/n) from Eq. (1). If we set wavelength λ_0 = 550 nm, refractive index n = 1.5 and clear aperture CA = 10 mm, the Fourier analysis of PSF with varying coding strength α and distance z_i is shown in Figure 4. Simulation demonstrates that the spot size is proportional to increasing alpha values and distances. While Figure 5 shows the Fourier transform with various different diameters when coding strength α = 50 and distance z_i = 50 mm. The PSF is inverse proportional to diameter. From the result of our simulation, we successfully verified and linked the geometric ray-tracing and Fourier analysis for cubic phase modulation.

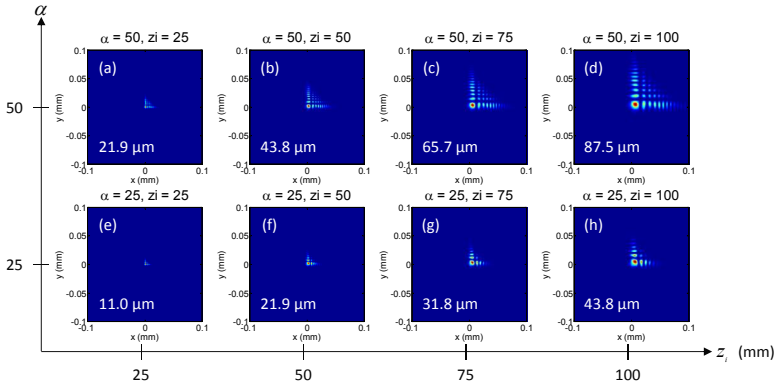

Figure 4. Simulation by Fourier analysis with different coding strength and distance z_i. Values calculated from geometric model are shown in the bottom left corner of each figure.

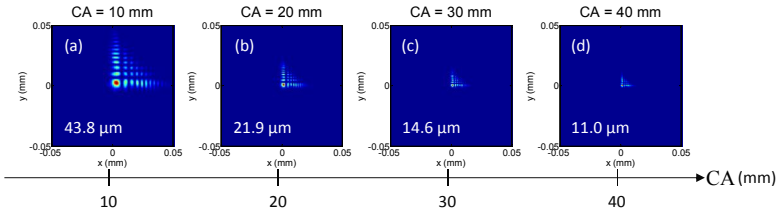

Figure 5. Simulation by Fourier analysis with different clear aperture. Values calculated from geometric model are shown in the bottom left corner of each figure.

2.4 Linear Shift Invariant Condition

The essential prerequisite of the pupil engineering is that the optical system must obey the property of linear shift invariance (LSI). Therefore, the phase modulation placed in pupil can be employed to manipulate PSF and MTF accordingly. For EDoF through amplitude or phase element, such as cubic phase mask, the PSF and MTF was designed to be less sensitive to defocus. However, the concept of pupil is a virtual aperture from the equivalent system. In practical operation, EDoF with phase pupil engineering might has some concerns: (1) exit pupil is at infinity (2) exit pupil is physically unavailable (3) structure and design issue in mechanism. In order to ease the EDoF operation, we usually put a phase element toward the end to manipulate the PSF. One of the difficulties lies in that different fields might have dissimilar PSFs. We performed two simulations to exhibit the influence of phase mask upon the PSF as well as Hilbert's space angle. Figure 6 (a-1) and (a-2) represents the coding on stop position and rear position, respectively. Three fields (0, 0.707 and 1) passed the phase element and each field crossed the same partial coding to satisfy the LSI condition. Figure 6 (b-2) shows the phase element on rear space, three fields passing the phase element subject to different coding resulting in dissimilar PSFs. Different field points must cross the same coding area to satisfy LSI condition in pupil engineering. In order to maintain the same PSFs for LSI condition, the aperture stop is the only one position that satisfied LSI condition (but not for all optical systems). All field points should pass through the same area with identical coding effect.

Hilbert's space angle is used to describe intensity correlation in Eq. (7) [8]. Hilbert's space angle is defined from 0 to 90 degrees to characterize the extended depth of focus, the smaller the angle, the more similar the PSF. Figure 6 (c-1) represents the Hilbert's space angle with aperture stop coding. Hilbert's space angle stays uniform at both on-axis and off-axis field for all object plane. On the other hand, as the case in coding on rear position in Figure 6 (c-2), severe change of PSF as well as Hilbert's space angle with different field angles would lead to a difficulty for the kernel design in the restoration process. More information will be lost and has a strong ringing effect afterward.

$$\cos\theta_H(y,z)=\frac{\sum I(y,z)\times I(0,0)}{\sqrt{I^2(y,z)}\sqrt{I^2(0,0)}} \tag{7}$$

In short, the position of the phase mask has a strong influence upon the EDoF system. The size and weighting factor of the phase mask are highly relevant to the system layout. In the following, we will propose a possible lens design for EDoF system and investigate the corresponding optimization scheme.

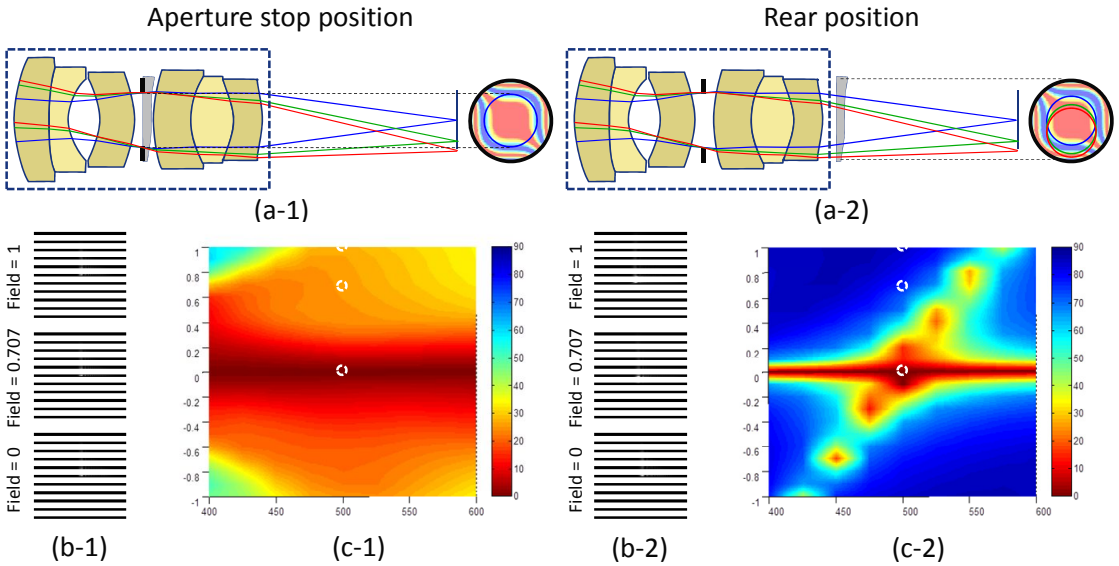

Figure 6. (a-1) coding on aperture stop position (a-2) coding on rear space position (b-1) different fields keep the same PSF shapes (b-2) different fields cause different PSF shapes (c-1) Hilbert's space angle is highly relevant for all field (c-2) The map of Hilbert's space angle is severely poor.

3. REAR PUPIL IMAGING SYSTEM

In this study, we attempt to simultaneously consider the lens design and phase mask for EDoF system rather than simply consider the mask on the pupil plane. The proper design of the optical system is likely to ensure high image fidelity with more tolerance in EDoF system. The choice of α should balance a trade-off between sharpness at the optimal focus position and the variation of the blur spot with respect to different object distances. In order to reduce lateral shift $T_p \approx 3(n-1)\lambda_0/2\pi n \times \alpha z_i/w$ and boost the MTF, we shall possibly decrease the distance z_i and enlarge the aperture size w. In the following, we compared two coding position in aperture stop imaging (ASI) and in rear pupil imaging (RPI), both satisfies the LSI condition. With different positions, even the same coding strength α of the phase mask will lead to a distinct difference.

3.1 ASI system

For mathematical convenience, we proposed a projection approach to find the coding effect in aperture stop imaging (ASI). From the characteristics of ambiguity function, extended range of EDoF is associated with coding strength α, where α is the inherent nature in EDoF system [5]. Therefore changing positions of phase mask will not affect the extended range of EDoF, but the size of PSF. Here we apply the concept of equivalent systems to find the solution. Coding on the aperture stop by coding strength α is equal to coding on the exit pupil of the equivalent system by the same α, but the coefficient A in equivalent system is changed. Equivalent exit pupil diagram of ASI system can be given by the image of the aperture stop in image space.

In Figure 7 (a), according to the properties mentioned above, the coding strength on the aperture stop is identical to the coding strength on the exit pupil of equivalent system. Coding strength $\alpha = 2\pi n A_1 w_1^3/\lambda_0 = 2\pi n A_2 w_2^3/\lambda_0$. The surface profile coefficient is $A_2 = A_1(w_1/w_2)^3$. The effective phase term can be written as

$$T_{p\_eff} = 3(n-1)[bfl + s(bfl/f - 1)]A_1 w_1^2 \tag{8}$$

where s is the distance from aperture stop to the rear lens, f is the focal length of rear lens, bfl is the distance from the rear lens to the image plane. The maximal coding strength can be determined by threshold 0.149 of MTF at Nyquist frequency.

3.2 RPI System

For rear pupil imaging (RPI) system, we aimed to design an EDoF system with maximal on-focus range and satisfy the LSI condition. To minimize Eq. (8) with respect to the variable s, the best solution is s equal to zero. It means the aperture stop is at the rear element, so-called rear pupil imaging (RPI) system as shown in Figure 7 (b). RPI system can utilize large coding strength α to acquire larger extended range with the same image quality, or vice versa, to utilize the same coding strength to get clearer image with the same extended range.

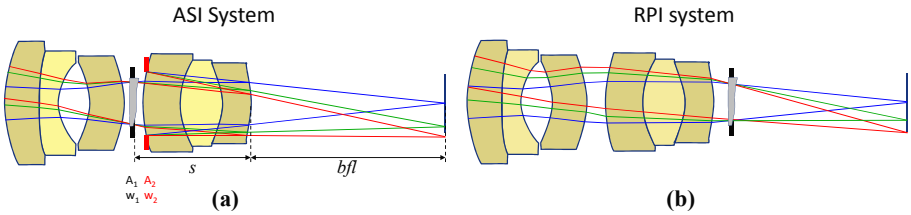

Figure 7. Illustrative configuration (a) coding on aperture stop position (b) coding on rear space position.

3.3 Simulation Results

Figure 8 illustrates the imaging chain associated with wavefront coded/decoded process. The original image is the perfect object image. After coded by a phase mask, PSF convolved with the ideal image and result in an intermediate image. Restoration process plays a key role in the wavefront coded photography. Much of the literature has

demonstrated that using different digital filters can restore the intermediate image in an extended depth of field of the whole imaging system. In our simulation a typical Wiener filter was used for restoration process.

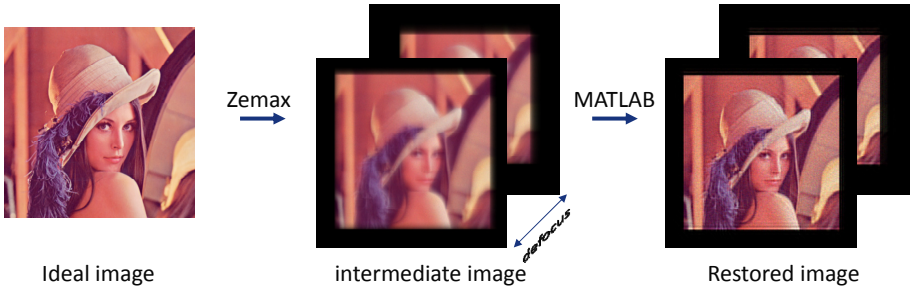

Figure 8. Imaging chain diagram associated with wavefront coded process by Zemax and decoded process by MATLAB program.

We designed an imaging system with the specifications of working f number 3.5, effective focal length 42 mm, magnification 0.54, and field of view 24°. In order to set threshold of MTF at Nyquist frequency larger than 0.149, we choose strength $\alpha = 50$ for our RPI and ASI systems. Figure 9 shows image performance of the ASI and RPI systems, respectively. The PSF of ASI system (70μm) is much larger than that of the RPI system (35μm). The intermediate blurred image by ASI system is more challenging to be resorted by the same coding factor and corresponding Weiner filter.

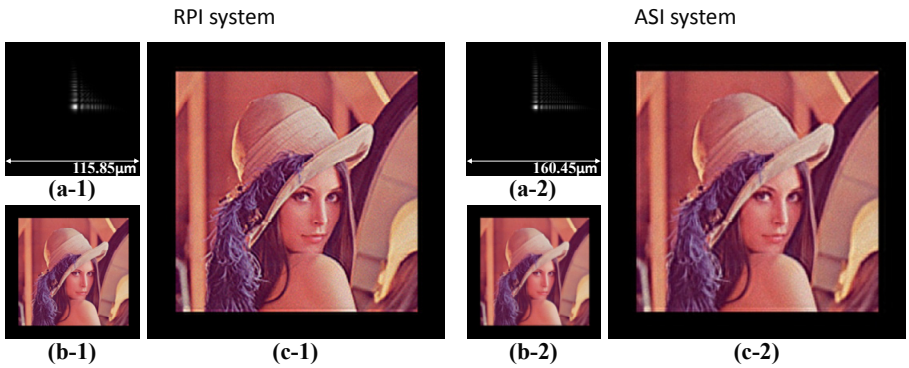

Figure 9. simulation results of RPI system and ASI system. (a-1) shows the width of PSF in RPI system is 35 μm, and (a-2) shows the width of PSF in ASI system is 70 μm (b) Blurred Images by wavefront coding and (c) de-blurred images by Wiener filter.

4. CONCLUSIONS

In this paper, the geometrical model of a cubic phase mask has been derived and linked to the conventional wave optics by Fourier analysis. For practical use in viewpoint of system design, pupil engineering is no longer validated in equivalent position amid an optical imaging system. In order to keep uniform phase coding satisfying the linear shift invariance, the position of the aperture stop should be re-examined. Rear pupil imaging (RPI) system, with shorter coding path, features small but more uniform coding effect, which leads to a stronger coding range of phase mask and system MTF. On the other hand, aperture stop imaging (ASI) is more sensitive to the different optical paths in the coding imaging system. With diverse coding effect subject to field view, the fidelity of restored image is hard to be kept along a wide range of depth of field. Compared with ASI system, RPI system is more likely to impose heavy coding to acquire huge extended range with same image requisite or utilize the same coding strength to get better image quality with same extended range. Meanwhile, the restoration process should consider the chromatic issue because the material refractive index is a function of wavelength.

5. ACKNOWLEDGMENT

This work was finically supported by National Science Council of Taiwan under contract no. NSC 101-2221-E-009 -113.

REFERENCES

[1] T. H. Lan, and C. H. Tien, "Manipulation of the steering and shaping of SPPs via spatially inhomogeneous polarized illumination," Opt. Express 18(22),23314-23323 (2010)
[2] Y. Xu, J. Singh, C. J. Sheppard, and N. Chen, "Ultra long high resolution beam by multi-zone rotationally symmetrical complex pupil filter," Opt. Express 15(10), 6409-6413 (2007)
[3] G. Toraldo di Francia, "Super-gain antennas and optical resolving power," Nuovo Cimento 9(3) suppl., 426-438 (1952)
[4] J. H. McLeod, "Axicons and their uses," J. Opt. Soc. Am. 50(2), 166-166 (1960)
[5] E. R. Dowski, and W. T. Cathey, "Extended depth of field through wavefront coding," Appl. Opt. 34(11), 1859-1866 (1995)
[6] S. S. Sherif, E. R. Dowski, and W. T. Cathey, "A logarithmic phase filter to extend the depth of field of incoherent hybrid imaging systems," Algorithms and Systems for Optical Information Processing V, 272-279 (2001)
[7] K. S. Kubala, E. R. Dowski, J. Kobus, and R. Brown, "Design and optimization of aberration and error invariant space telescope systems," Proc. SPIE 5524, 54-65 (2004)
[8] S. S. Sherif, W. T. Cathey, and E. R. Dowski, "Phase plate to extend the depth of field of incoherent hybrid imaging systems," Appl. Opt. 43(13), 2709-2721 (2004)
[9] J. W. Goodman, [Introduction to Fourier optics], 3rd ed., Roberts & Co., Englewood, Colo., (2005)
[10] B. E. A. Saleh, and M. C. Teich, [Fundamentals of photonics], 2nd ed., Wiley-Interscience, Hoboken, N.J. (2007)
[11] R.C. Gonzalez, R. E. Woods, and S. L. Eddins, [Digital image processing using MATLAB], Pearson Prentice Hall, Upper Saddle River, N. J. (2004)